NASA Technical Memorandum 81863

Dynamic Response of a Forward-Swept-Wing Model at Angles of Attack up to 15° at a Mach Number of 0.8

Robert V. Doggett, Jr., and Rodney H. Ricketts

NOVEMBER 1980

NASA

NASA Technical Memorandum 81863

Dynamic Response of a Forward-Swept-Wing Model at Angles of Attack up to 15° at a Mach Number of 0.8

Robert V. Doggett, Jr., and Rodney H. Ricketts
Langley Research Center
Hampton, Virginia

National Aeronautics
and Space Administration

**Scientific and Technical
Information Branch**

1980

Request List

Produced Wednesday, February 16, 2000 at 2:30 AM

1) Request ID: REQ-23590
Request Type: GALAXIEREQ
Date Placed: 2/15/2000
Reply Date: NEVER
Origin Library: LANGLEY

Status: NEW
Operator Access: LANPUB
Date Modified: NEVER
Date Viewed: NEVER
Service Library: LANGLEY

User ID: 180557
User Name: Florance, James

Call Number: NASA-TM-81863
Item ID: 3117600518047?
Report number:81N12448
Personal author:Doggett, Robert V., Jr.
Corporate author:NASA LaRC
Title:Dynamic response of a forward-swept-wing model at angles of attack up to 15 degrees at a Mach number of 0.8.
Publication info:80/11/00; 28 p.

REQUEST INFORMATION ---
mail stop *required*:340

filled
2/16/2000

SUMMARY

The effects of angles of attack up to 15° on the dynamic response of a wing model swept forward 44° have been determined experimentally at a Mach number of 0.8. The semispan wing with a panel aspect ratio of 1.77 was constructed of composite material and was a 0.6-size, dynamically scaled, aeroelastic model of a proposed flight-demonstrator airplane. Dynamic bending moments are presented for three values of dynamic pressure. These data included both broad-band responses and individual responses in the first two natural modes. Total damping ratios are presented for the response in the first two natural modes.

The results showed that the dynamic response increased with increasing angle of attack with a peak value occurring at an angle of attack near 13°. At angles of attack other than those near 13°, the response had characteristics usually attributed to buffeting and was similar to that often observed for aft-swept wings. Although the response at an angle of attack near 13° was similar to buffeting, this response also had characteristics sometimes seen when a dynamic instability is being approached. No instability was found, however, over the range of parameters investigated.

INTRODUCTION

Although it has been recognized for some time that forward-swept wings may offer some aerodynamic advantages over aft-swept wings, forward-swept wings have not been considered seriously in new airplane designs in the United States because of the mass penalty required to satisfy static-divergence constraints (ref. 1). That is, the additional structural mass required to provide sufficient stiffness for divergence prevention more than offsets aerodynamic-performance benefits of forward sweep. Although this situation is still true for wings of conventional metal construction, it may not be the case for wings constructed of composite materials. Analytical studies (ref. 2, for example) show that the divergence speed of a composite structure can be increased to a satisfactory value without having to add a large amount of structural mass to a strength-designed structure. This increase is accomplished by arranging the composite lamina (aeroelastic tailoring) to reduce the washin that occurs as aerodynamic loading is increased.

With composite structural technology offering a practical solution to the divergence problem, interest has been kindled in the use of forward-swept wings, in particular, in applications to high-performance military airplanes. This renewed interest was confined initially to analytical studies, but recently it has been expanded to include wind-tunnel model studies to verify analytical predictions. In one of these wind-tunnel studies a 0.6-size, dynamically scaled, aeroelastic semispan model of a proposed flight-demonstrator-airplane wing was designed and built by Rockwell International under contract to the U.S. Air Force and was tested by the National Aeronautics and Space Administration in the

Langley Transonic Dynamics Tunnel. These tests were conducted in close coordination with the Defense Advanced Research Projects Agency (DARPA) which is providing considerable impetus to the development of forward-swept-wing technology. The general purpose of these wind-tunnel tests was to determine the aeroelastic characteristics of a realistic, aeroelastically tailored, forward-swept-wing configuration constructed of composite material. A specific purpose, which is the subject of this paper, was to determine whether the model exhibited any unusual dynamic response as a function of angle of attack. Currently, there is concern about angle-of-attack effects on aeroelastic response and instabilities because of unpublished results from both recent flight tests of an advanced bomber airplane and wind-tunnel model tests of a highly maneuverable fighter configuration, and because of published results from other configurations. (For example, see refs. 3 and 4.)

Exploratory studies were made to determine dynamic response over a range of angles of attack at several subsonic Mach numbers. Although model response did increase with angle of attack at several Mach numbers, the largest response was obtained in the vicinity of a Mach number of 0.8. Consequently, this Mach number was chosen for additional study, and the results are reported herein. Dynamic bending moments for three values of dynamic pressure are presented as a function of angle of attack. These data include both narrow-band response in the first two natural modes and broad-band response. In addition, total damping ratios are presented for the responses in the first two natural modes.

SYMBOLS

Measurements and calculations were made in U.S. Customary Units and are presented in both the International System of Units (SI) and U.S. Customary Units.

A	wing area
C_b	static bending-moment coefficient, $M_{b,s}/qAc$
C_β	buffet moment coefficient, $M_{b,rms}\gamma^{1/2}/qAc$
c	wing average chord
f	frequency
g	structural damping coefficient, $2\gamma_{st}$
M	Mach number
$M_{b,d}$	dynamic bending moment
$M_{b,s}$	static bending moment
$M_{b,rms}$	root-mean-square (rms) bending moment
q	dynamic pressure

α angle of attack

γ total damping ratio, $\gamma_a + \gamma_{st}$

γ_a aerodynamic damping ratio

γ_{st} structural damping ratio, g/2

ρ fluid density

$\Phi(f)$ normalized autospectrum

Subscripts:

1 first natural mode

2 second natural mode

APPARATUS AND PROCEDURE

Wind Tunnel

This investigation was conducted in Freon[1] 12 in the Langley Transonic Dynamics Tunnel. This facility is a slotted-throat, single-return wind tunnel that has a 4.88-m-square (16-ft) test section with cropped corners. The stagnation pressure can be varied from slightly above atmospheric to near vacuum, and the Mach number can be varied from 0 to 1.2. The tunnel is of the continuous-operation type and is powered by a motor-driven fan. Both test-section Mach number and density are continuously controllable.

Model

General.- The semispan wind-tunnel model used was a 0.6-size, dynamically scaled, aeroelastic wing of a proposed forward-swept-wing, flight-demonstrator airplane that has been aeroelastically tailored by using composite materials to satisfy divergence, flutter, and strength constraints. A photograph of the model mounted in the wind tunnel is shown in figure 1. A line drawing showing model geometry is presented in figure 2. The model was designed to match the nondimensional scaling parameters of Mach number, reduced frequency, and mass ratio for the airplane flying at sea level (q = 70.86 kPa (1480 lbf/ft^2)) at M = 1.0. Corresponding wind-tunnel conditions are M = 1.0, ρ = 0.427 kg/m^3 (0.000828 slug/ft^3), and q = 5.42 kPa (113.2 lbf/ft^2). The model had a panel aspect ratio of 1.77, a semispan of 1.6325 m (64.272 in.), a taper ratio of 0.46, and a leading-edge forward-sweep angle of 44°. The airfoil section at

[1]Freon: Registered trademark of E. I. du Pont de Nemours & Co., Inc. Use of trade names does not constitute an official endorsement, either expressed or implied, by NASA.

the root was an NACA 64A004.4 which linearly tapered to an NACA 64A003.2 at the tip. The model wing was untwisted. The model root was mounted off the tunnel wall so that the entire wing was outside the wind-tunnel-wall boundary layer. A splitter plate was used to provide a reflection plane at the model root. The model was attached to a remotely controlled turntable mounted flush with the wind-tunnel wall so that angle of attack could be changed during the tests.

Construction.- The primary structure was made of graphite epoxy skins bonded to a polyurethane foam core with internal fiberglass ribs and spars which formed a wing box that contributed practically all of the model stiffness. The general arrangement of the main ribs and spars is shown in figure 3. Along the leading and trailing edges and at the tip the foam core was covered with fiberglass skins which overlapped the graphite skin to provide structural continuity in the wing skins. The arrangement of the graphite lamina (ply direction) was the same on the model as for the full-scale design, although the number of lamina in a given direction was different. The ply directions were 9°, 30°, 90°, and 139°, measured clockwise from the model root chord when viewed from above. Most of the lamina were oriented in the 30° direction. The relative lengths of the arrows in figure 3 are indicative of the average number of plies in the four directions outboard of the kick rib. An aluminum-alloy rib and fittings were provided at the root chord to provide a means of attaching the model to a steel mounting fixture which was attached to the wind-tunnel sidewall turntable. The bending and torsional stiffness of the mounting fixture simulated the flexibility of the wing carry-through structure and fuselage of the full-sized airplane. To simulate mass and mass distribution, ballast weights were imbedded and glued in the foam core of the model.

Physical properties.- The model weighed 16.19 kg (35.70 lbm). Measured natural frequencies, node lines, and structural damping coefficients for the first six vibration modes are presented in figure 4. The first, second, fifth, and sixth modes are primarily bending modes. The third mode is a coupled bending-torsion mode, whereas the fourth mode is primarily torsion in character.

Instrumentation.- The model was instrumented with eight resistance wire strain-gage bridges. The primary bending-moment strain gage was located just outboard of the kick rib as indicated in figure 3. This gage was calibrated to measure bending moment and was used to obtain the dynamic-response data presented in this report. The orientation of the gage was such that it was virtually insensitive to torsional strains. The other seven gages were located at critical points on the model and were used to monitor loads and stresses to ensure that design-limit loads were not exceeded during testing.

Test Procedure

The determination of a particular set of data proceeded in the following manner. With the model set at a low positive angle of attack, the tunnel speed was increased until the desired test Mach number was reached. It was ensured that the desired dynamic pressure would be reached at this Mach number by evacuating the tunnel to a prescribed total pressure prior to starting the wind-tunnel fan. Once the wind-tunnel flow conditions had stabilized, the output

signals from the strain gages were recorded on analog tape and monitored on recording oscillographs. In addition, the strain-gage signals were routed through analog-to-digital converters to the digital computer of the wind-tunnel data-acquisition system. (The features and capabilities of the data-acquisition system are discussed in ref. 5.) The means and root-mean-square values of the digitized data signals were calculated, tabulated, and displayed to the test engineer. A 30-sec time history of the bending-moment strain-gage signal was recorded on digital tape at 300 samples per second for off-line data reduction. The digital signal was converted to engineering units prior to recording. Once sufficient data had been obtained at the initial angle of attack, the angle of attack was increased slowly to a higher value. While the angle of attack was being changed, the strip charts were monitored visually and the peak loads (static plus dynamic) on the model, which were being updated continuously by the digital computer, were monitored to ensure that allowable loads were not exceeded. Once the second angle of attack was reached, data were recorded and processed. The angle-of-attack stepping process was repeated until data had been obtained over the range of interest. Data at other dynamic pressures were obtained by increasing the tunnel pressure by bleeding Freon 12 into the wind tunnel through an expansion valve until the desired value of dynamic pressure was reached and then by repeating the angle-of-attack stepping process.

Test Conditions

Exploratory studies were conducted over a range of angles of attack at several subsonic Mach numbers. Because the largest response occurred near $M = 0.8$, this Mach number was selected for detailed study. Specifically, data were obtained at $M = 0.8$ for angles of attack up to about 15° for three nominal values of dynamic pressure: 0.397 kPa (8.3 lbf/ft^2), 0.570 kPa (11.9 lbf/ft^2), and 0.709 kPa (14.8 lbf/ft^2). Reynolds numbers based on wing average chord at these dynamic pressures are 0.50×10^6, 0.73×10^6, and 0.89×10^6, respectively.

For the tests at Reynolds numbers of 0.50×10^6 and 0.89×10^6 the model was equipped with transition strips (No. 46 carborundum grit) having a width of about 0.025 chord and located along the 5-percent chord on both the upper and lower surfaces. For the results reported herein for a Reynolds number of 0.73×10^6, the transition strips were removed. However, based on a limited amount of data (not presented herein) obtained with and without transition strips over the range of the higher Reynolds numbers, it is believed that the results obtained at Reynolds numbers of 0.73×10^6 and 0.89×10^6 would be the same whether or not transition strips were present. No data were obtained at the lowest Reynolds number for comparison.

DATA REDUCTION

The dynamic-response data were obtained by off-line processing the digitized time history of the bending moment recorded at each test point. The digital-analyses methods used were standard state-of-the-art techniques. (See, for example, ref. 6.)

The static bending moment (mean value of signal) was determined for each test condition. For each time history the mean was determined for several record lengths (the shortest being 3 sec) to determine whether a meandering mean was present. None was found. The mean was subtracted from each record prior to additional processing.

Broad-band (0 to 150 Hz) root-mean-square (rms) values and autospectra (power spectral densities) were calculated for each test condition. The time histories were passed through a band-reject recursive filter to remove 60-cycle noise prior to obtaining the broad-band rms values and the autospectra. The rms response in the first mode (about 7 Hz) and second mode (about 20 Hz) was obtained by filtering the time histories with narrow-band recursive digital filters. The transfer functions of the filters are shown in figure 5. The rms response was obtained by analyzing the filtered data.

The total damping in the first and second modes was determined by applying the random decrement (randomdec) subcritical response method (ref. 7) to the filtered time histories. The randomdec method provides a means of determining the step response of a system that is excited by a random force. This is accomplished by performing an ensemble average of segments of the response time history. The resulting step response is called the randomdec signature. Typical randomdec signatures are presented in figure 6. Because the randomdec signature is an approximation to the step response and because each time history has been filtered to obtain response in only one mode, the damping could be determined from the log decrement of the decaying oscillation. A least-squares method was used to fit the envelope of the decaying oscillation. The damping was obtained from the fitted curve. The frequency of oscillation was obtained from the average time between peaks in the signal.

RESULTS AND DISCUSSION

Exploratory studies were conducted for the forward-swept-wing model over a range of angles of attack at several subsonic Mach numbers to determine whether any significant dynamic response existed that was sensitive to angle of attack. The largest response was obtained near $M = 0.8$. This Mach number was selected for more detailed study, and results obtained are presented and discussed in this section.

Broad-Band Response

In general, the dynamic response appeared to be that of a lightly damped, multi-degree-of-freedom system driven by random excitation. That is, the response appeared to be a combination of sinusoids of constant frequency and randomly varying amplitude, each sinusoid being a response in a natural-vibration mode. An illustrative time history for $\alpha = 8^{\circ}$ is presented in figure 7(a). This type of response was observed throughout the studies of the angle-of-attack range, except near $\alpha = 13^{\circ}$ where the dynamic response was at a maximum. At this angle of attack the response appeared more like that of a single-degree-of-freedom system. An illustrative time history for $\alpha = 13^{\circ}$ is presented in figure 7(b). Although the amplitude of the response appears gen-

erally to be random, the time history does have some characteristics seen in response time histories when a dynamic instability is being approached, in particular, the somewhat sustained bursts of relatively large response.

rms response.- The variation of broad-band (0 to 150 Hz) rms bending moment is presented in figure 8 for three dynamic-pressure values. The trends of the data for different dynamic pressures are the same, but the level of the response increases with dynamic pressure. The data show a gradual increase in bending moment as angle of attack increases from 0° to 12°. At $\alpha = 12^\circ$ the bending moment increases rapidly to a peak value near $\alpha = 13^\circ$, then decreases followed by a subsequent increase as angle of attack is increased further.

Although the rms bending moment at $\alpha = 13^\circ$ is considerably larger than that at low angles of attack, it is small compared to the static bending moment. For example, at $\alpha = 13^\circ$ for $q = 0.709$ kPa (14.8 lbf/ft^2) the rms moment is only about 5 percent of the static moment. If a peak dynamic moment of three times the rms value (0.993 confidence for a normal random process) is assumed, the maximum dynamic moment is about 15 percent of the static moment, or about 13 percent of the total moment (static plus dynamic).

Frequency content.- Some representative normalized autospectra of the dynamic bending moment are presented in figure 9 for several angles of attack. These spectra are for $q = 0.709$ kPa (14.8 lbf/ft^2), but they are typical of results for the other dynamic pressures. Although the frequency range of the autospectra was from 0 to 150 Hz, the spectra are plotted only to 60 Hz because modes above the fifth (55 Hz) did not contribute appreciably to the response. The autospectra are normalized by the first-mode response (the largest contributor) so that the relative contribution of each mode can be seen readily. (Autospectrum amplitude is proportional to the square of the response. For example, a value of normalized spectrum amplitude equal to 0.5 for, say, the second mode indicates that the rms response in the second mode is 0.707 times as large as the rms response in the first mode.)

The autospectra show clearly that the dynamic response was composed primarily of response in the first and second natural modes. The largest response was in the first mode throughout the angle-of-attack range. Although third- and fifth-mode responses are present, their levels are low when compared to the first-mode response. The autospectra show no response in the fourth mode (51 Hz) because the strain gage was insensitive to torsional strains. During the tests examination of time histories from other gages that were sensitive to torsional strains indicated very little response in the fourth mode. The relative contribution of the second mode changes with angle of attack. At $\alpha = 10^\circ$, 12°, and 15°, the second-mode response is almost as large as the first-mode response. At other angles of attack the second-mode response is considerably smaller. At $\alpha = 13^\circ$, the response is almost totally composed of first-mode response.

A comparison of the frequencies at which peaks occur in the autospectra with the wind-off natural frequencies in figure 4 indicates that the aerodynamic forces had little effect on the natural frequencies of the model. Wind-on frequencies are approximately equal to wind-off frequencies.

Static Bending Moment

Bending of the large increase in response that occurred near $\alpha = 13^{\circ}$, the static bending moment was examined to see if any changes occurred in the vicinity of $\alpha = 13^{\circ}$. The variation of static bending-moment coefficient C_b with angle of attack is shown in figure 10. Data are presented for the three dynamic-pressure levels. The variation of C_b with α is smooth for all three dynamic pressures. It would be expected that any abrupt changes in steady-state aerodynamic characteristics such as lift-curve slope and center-of-pressure location would show up as a change in C_b. Because none was found, it was concluded that there were no abrupt changes in the steady aerodynamic characteristics. It is to be noted, however, that over the angle-of-attack range from 0° to 12° the rate of change of C_b (slope of curve) is increasing. At about $\alpha = 12^{\circ}$ the slope, although still positive, does begin to decrease which may indicate the beginning of shock-induced separation.

Although some of the differences in C_b at a given angle of attack may be due to Reynolds number effects, it is believed that static aeroelastic effects are the primary cause of the differences. Even though the wing was tailored to reduce washin (increase in outboard angles of attack caused by elastic deformations), some washin does occur. This causes the static bending moment to be larger as dynamic pressure is increased.

Narrow-Band Response

First mode.- The variation of the rms bending moment in the first natural mode with angle of attack is presented in figure 11. The trend of these data is similar to that found for the broad-band response shown in figure 8. The first-mode response gradually increases until an angle of attack of about 12° is reached. At $\alpha = 12^{\circ}$ the response increases sharply to a maximum value near $\alpha = 13^{\circ}$ and then decreases at higher angles of attack. The highest response occurs at the highest dynamic pressure.

The variation of the total damping for the first mode (structural plus aerodynamic) with angle of attack is presented in figure 12. In general, the damping is larger at the higher dynamic pressures. The trends of the data are similar for the three dynamic-pressure levels. A peak damping value occurs at about $\alpha = 12^{\circ}$ and is followed by a decrease to a minimum value at about $\alpha = 13^{\circ}$, where the maximum response occurs, and then is followed by another increase.

Dynamic analysis of buffeting (see ref. 8, for example) shows that the rms response is directly proportional to the dynamic pressure and inversely proportional to the square root of the total damping. Therefore, if the wing response is due to buffeting, the data at the three dynamic-pressure levels should correlate by using a buffet moment coefficient C_β which is a product of the rms bending moment and the square root of the total damping ratio divided by the product of dynamic pressure, wing area, and average chord. For the first mode the variation of $C_{\beta,1}$ with angle of attack is presented in figure 13. Over the angle-of-attack range from 0° to about 10° the data are brought together by using the parameter $C_{\beta,1}$. At angles of attack from about 10° to 15° the

results for $q = 0.570$ kPa (11.9 lbf/ft^2) and $q = 0.709$ kPa (14.8 lbf/ft^2) agree very well but differ from the results for $q = 0.397$ kPa (8.3 lbf/ft^2). The Reynolds number at $q = 0.397$ kPa (8.3 lbf/ft^2) was very low, about 0.5×10^6. Reynolds number effects may be the reason why the lowest dynamic-pressure data do not correlate better with the results for other dynamic pressures.

Based on the response at the two higher dynamic pressures, it is concluded that the response was of the buffet type throughout the angle-of-attack range and was similar to buffet characteristics often observed for aft-swept wings. See reference 9, for example. The disagreement of the data for the lowest dynamic pressure near $\alpha = 13^\circ$, however, adds some uncertainty to this conclusion. This disagreement combined with the sharp reduction in damping that occurs near $\alpha = 13^\circ$ (see fig. 12) may indicate that a dynamic instability is being approached.

Second mode.- The variation of rms bending moment in the second natural mode with angle of attack is presented in figure 14. In general, the response gradually increases with increasing angle of attack. Although there is no peak in the response at $\alpha = 13^\circ$ similar to that found for the first mode (see fig. 11), there is, however, evidence of the beginning of a peak in the response in the range of α from 14° to 15°.

The variation of total damping for the second mode with angle of attack is presented in figure 15. Up to an angle of attack of about 12° the total damping ratio is approximately equal to the structural value $\gamma_{st} = 0.0075$, indicating that the aerodynamic forces add little aerodynamic damping for this mode. In the angle-of-attack range from 12° to 15° the total damping has an increasing trend, thus showing that the aerodynamic forces produce a measurable amount of damping.

The variation of the buffet moment coefficient $C_{\beta,2}$ for the second mode with angle of attack is presented in figure 16. In this case the correlation is good for all three dynamic pressures, thus indicating that the second-mode response was probably caused by buffet flow.

CONCLUDING REMARKS

The effects of angles of attack up to 15° on the dynamic response of a wing model swept forward 44° have been determined experimentally at a Mach number of 0.8. The aspect-ratio-1.77 wing was constructed of composite material and was a 0.6-size semispan, dynamically scaled, aeroelastic model of a proposed flight-demonstrator airplane. Dynamic bending moments have been presented for three values of dynamic pressure. These data included broad-band responses and individual responses in the first two natural modes. Total damping ratios were presented for the response in the first two natural modes.

The results showed that the dynamic response increased with increasing angle of attack with a peak value occurring at an angle of attack near 13°. At angles of attack other than those near 13°, the response had characteris-

tics usually attributed to buffeting and was similar to that often observed for aft-swept wings. Although the response at an angle of attack near 13° was similar to buffeting, this response also had characteristics sometimes seen when a dynamic instability is being approached. No instability was found, however, over the range of parameters investigated.

Langley Research Center
National Aeronautics and Space Administration
Hampton, VA 23665
October 3, 1980

REFERENCES

1. Forward-Swept Wing Potential Studied. Aviat. Week & Space Technol., vol. 110, no. 5, Jan. 29, 1979, pp. 126-127.

2. Krone, Norris J., Jr.: Divergence Elimination With Advanced Composites. AIAA Paper No. 75-1009, Aug. 1975.

3. Erickson, Larry L.: Transonic Single-Mode Flutter and Buffet of a Low Aspect Ratio Wing Having a Subsonic Airfoil Shape. NASA TN D-7346, 1974.

4. Moss, G. F.; and Pierce, D.: The Dynamic Response of Wings in Torsion at High Subsonic Speeds. Unsteady Airloads in Separated and Transonic Flow, AGARD-CP-226, 1977, pp. 4-1 - 4-21.

5. Cole, Patricia H.: Wind Tunnel Real-Time Data Acquisition System. NASA TM-80081, 1979.

6. Otnes, Robert K.; and Enochson, Loren: Digital Time Series Analysis. John Wiley & Sons, Inc., c.1972.

7. Cole, Henry A., Jr.: On-Line Failure Detection and Damping Measurement of Aerospace Structures by Random Decrement Signatures. NASA CR-2205, 1973.

8. Huston, Wilber B.: A Study of the Correlation Between Flight and Wind-Tunnel Buffet Loads. AGARD Rep. 111, Apr.-May 1957.

9. The Effects of Buffeting and Other Transonic Phenomena on Maneuvering Combat Aircraft. AGARD-AR-82, 1975.

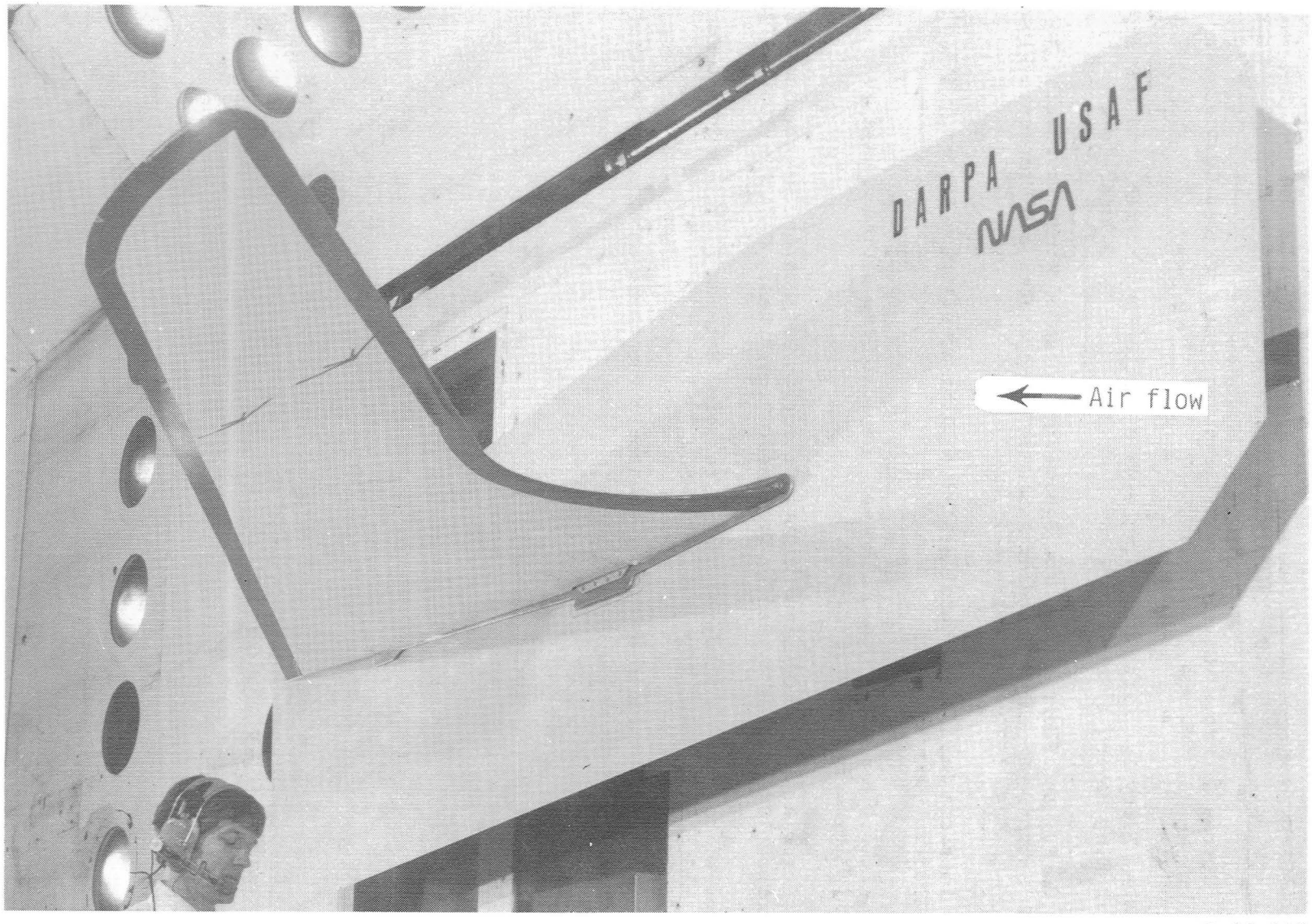

L-80-196

Figure 1.- Photograph of model mounted in wind tunnel.

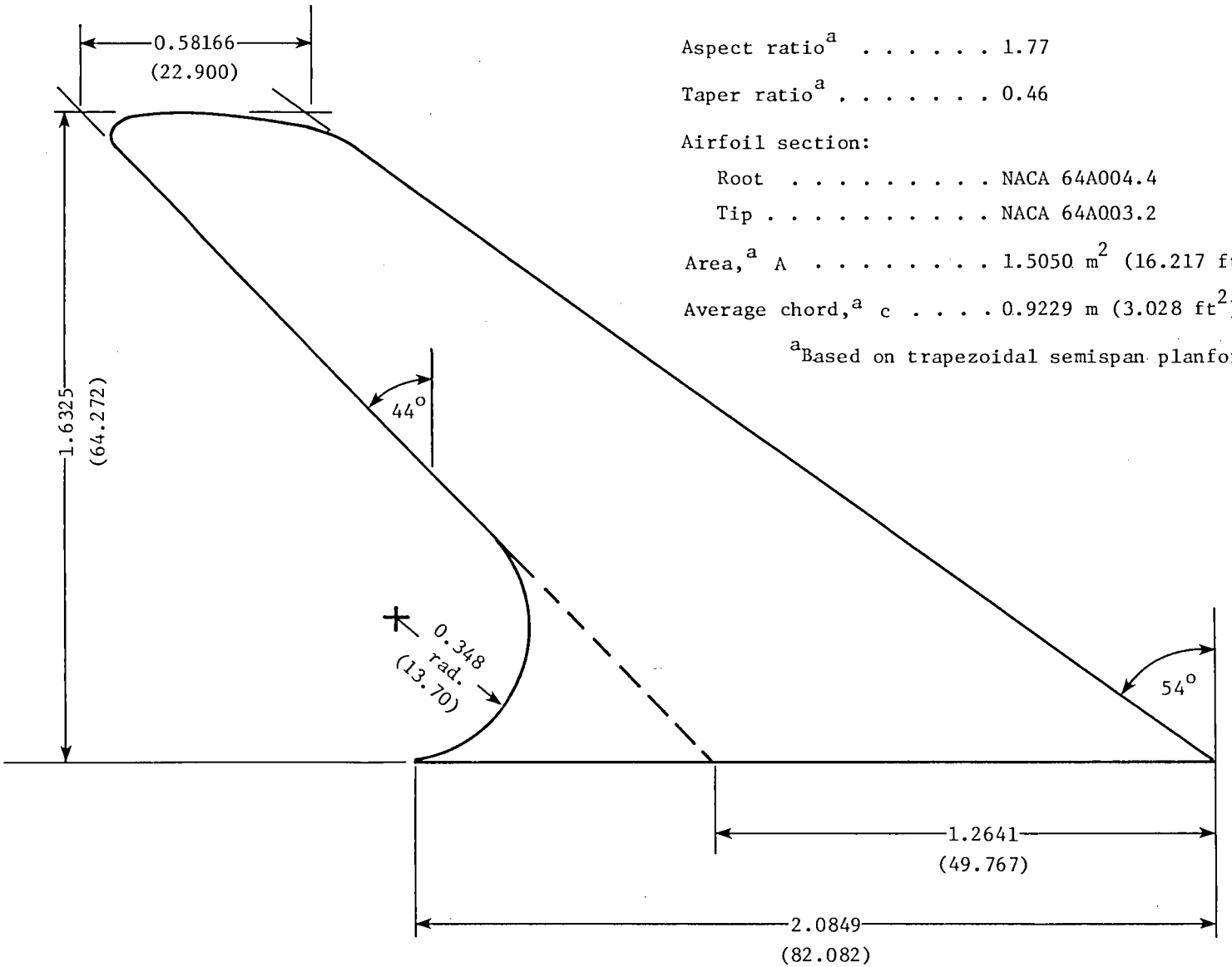

Aspect ratio[a] 1.77

Taper ratio[a] 0.46

Airfoil section:

Root . . . . . NACA 64A004.4

Tip . . . . . NACA 64A003.2

Area,[a] A . . . . . 1.5050 m^2 (16.217 ft^2)

Average chord,[a] c . . . . 0.9229 m (3.028 ft^2)

[a]Based on trapezoidal semispan planform.

Figure 2.- Model geometry. Linear dimensions are given in meters (inches).

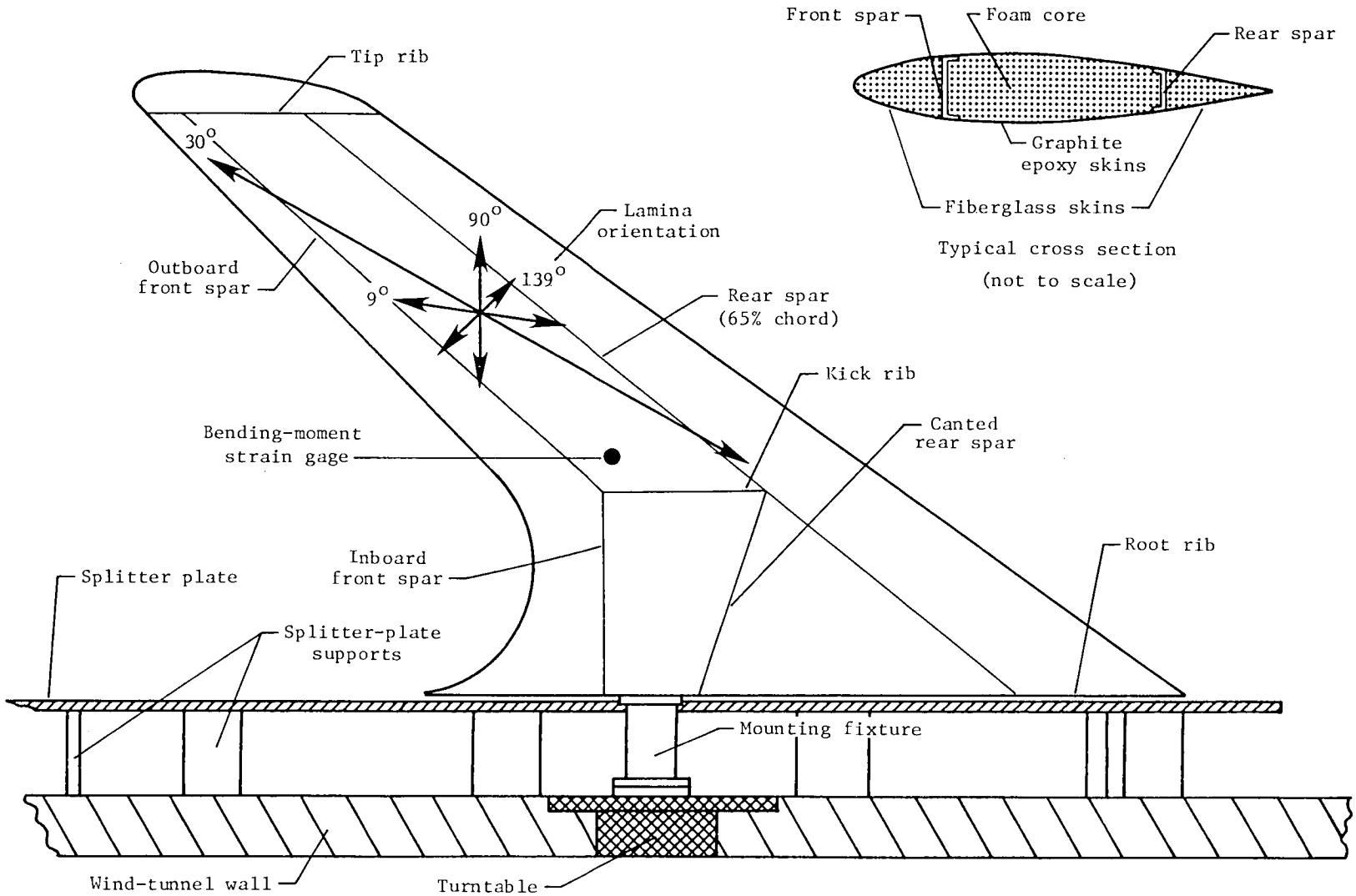

Figure 3.- Structural arrangement.

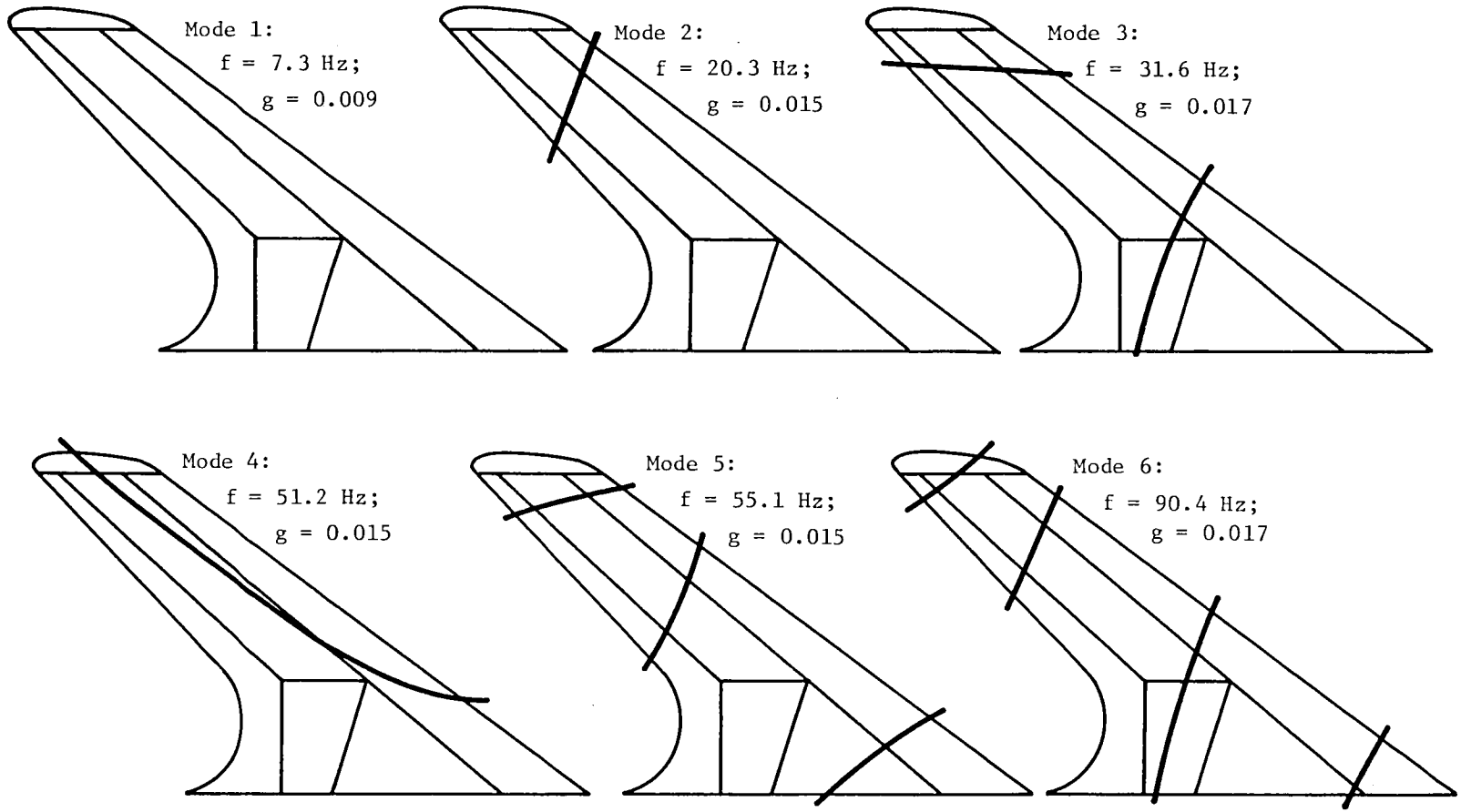

Figure 4.- Measured natural frequencies, structural damping coefficients, and node lines.

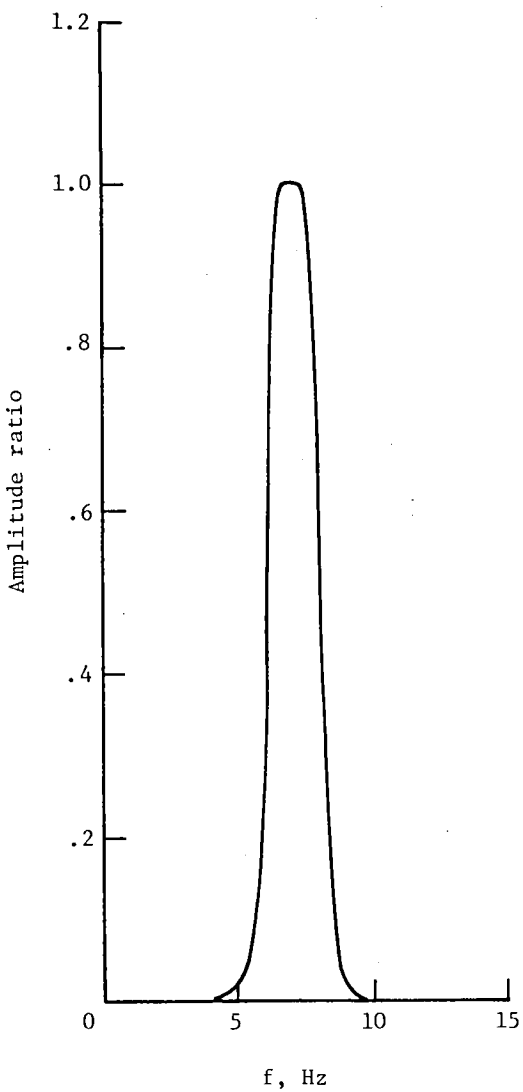

(a) First mode.

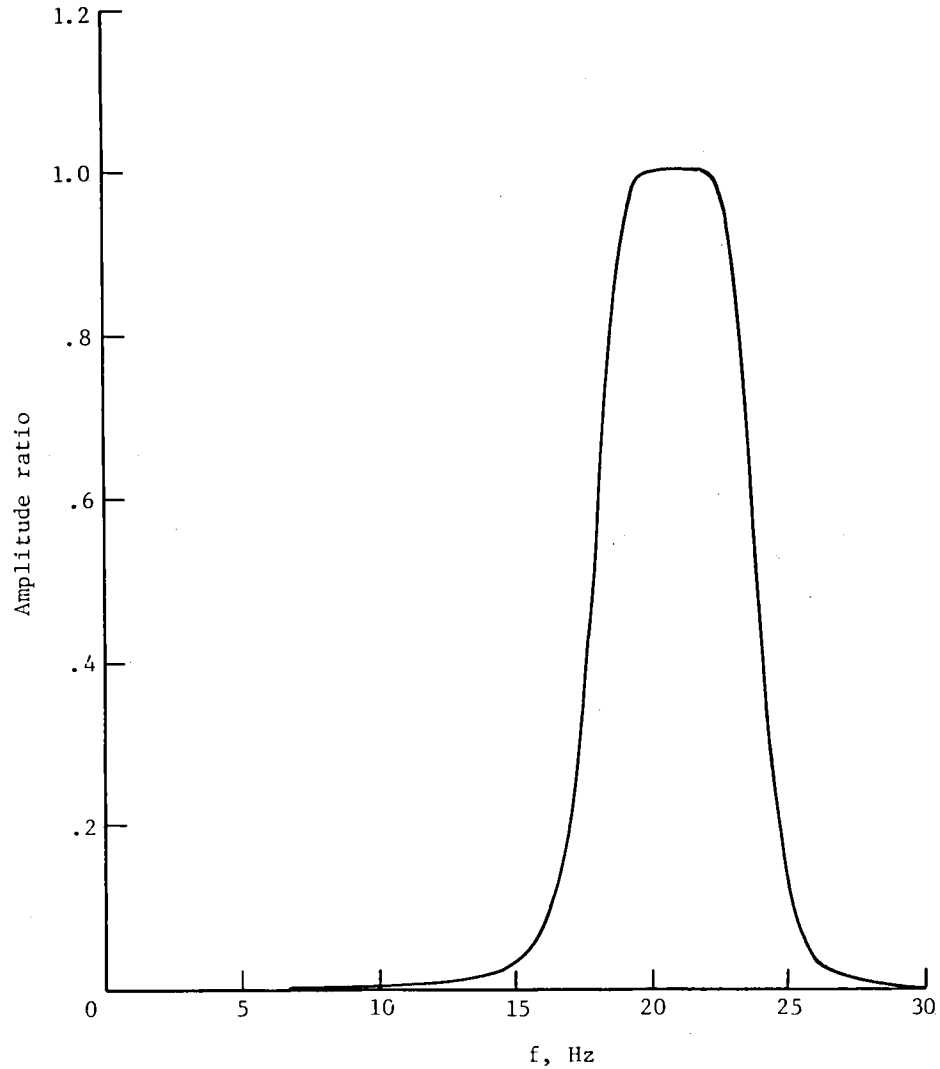

(b) Second mode.

Figure 5.- Digital-filter transfer functions.

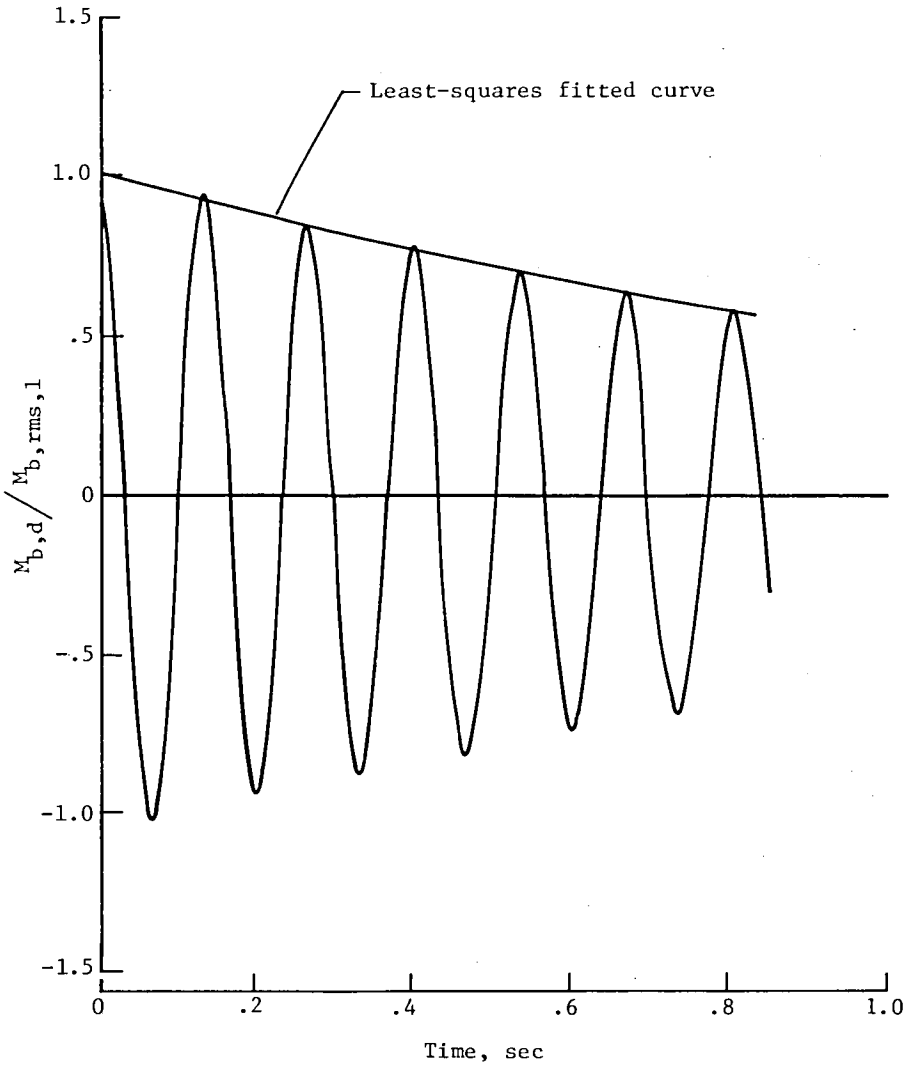

(a) First mode.

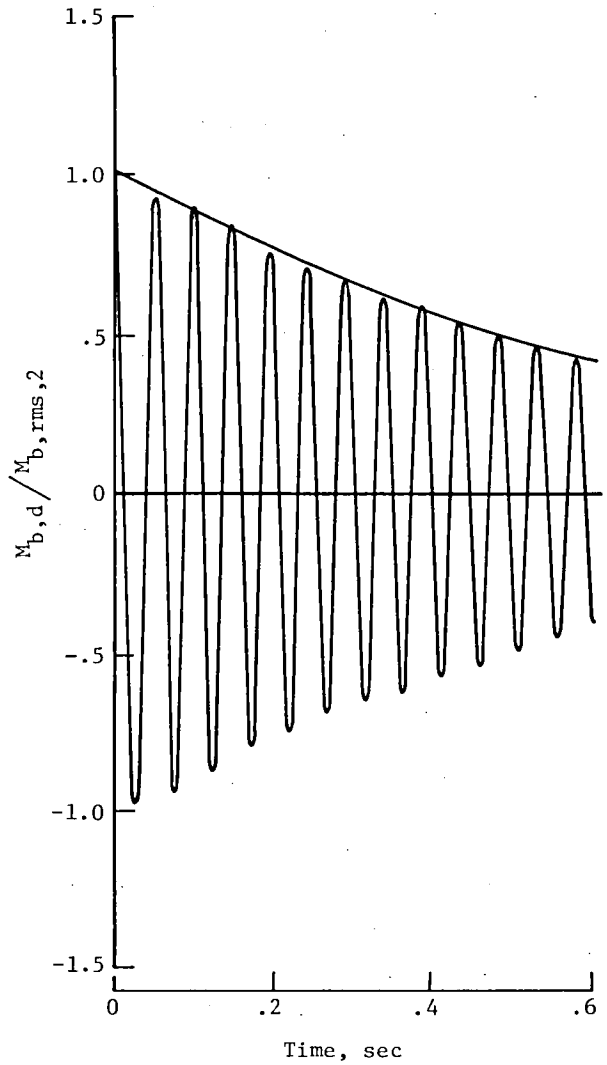

(b) Second mode.

Figure 6.- Representative randomdec signatures.

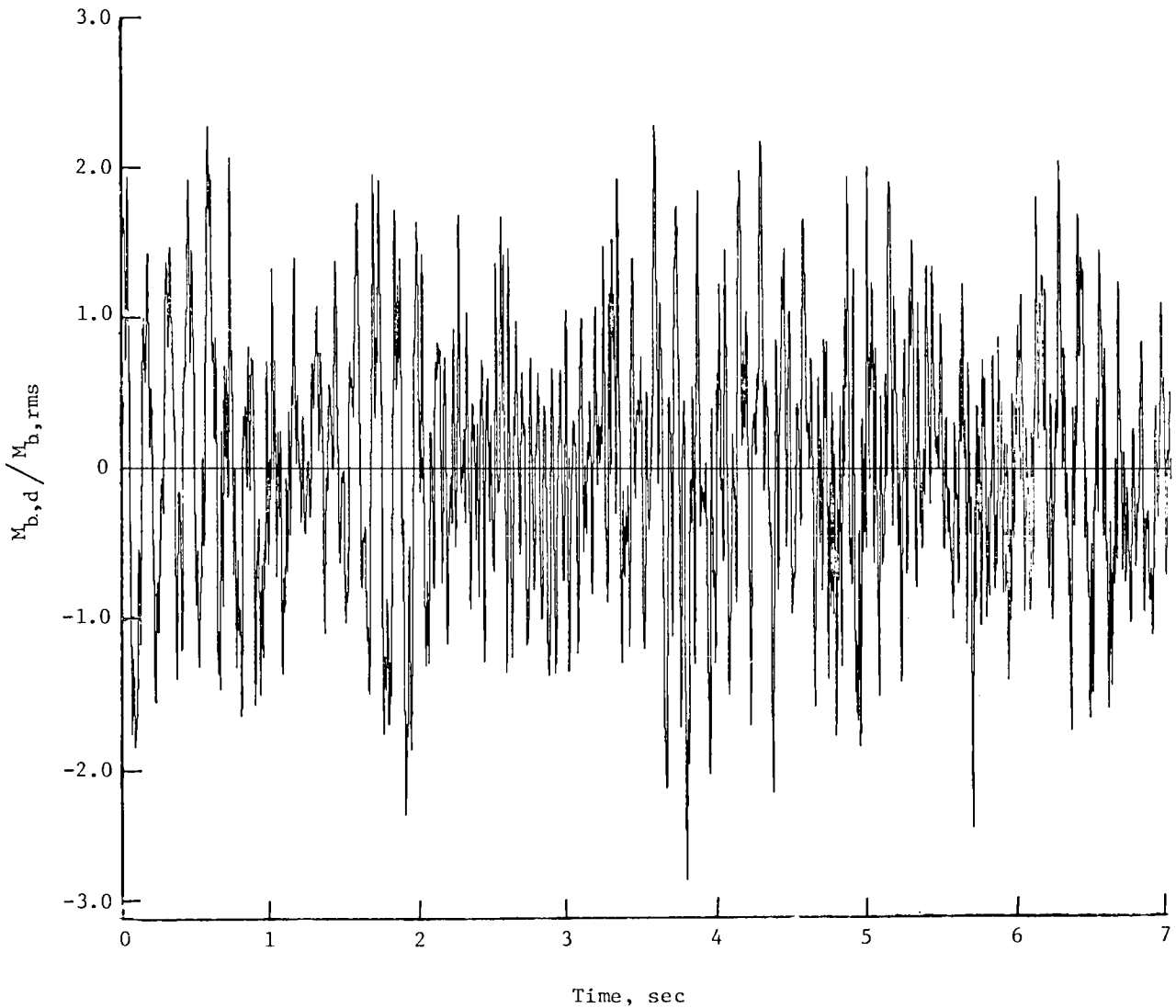

(a) $\alpha = 8^{o}$.

Figure 7.- Illustrative time histories. q = 0.709 kPa (14.8 lbf/ft^2).

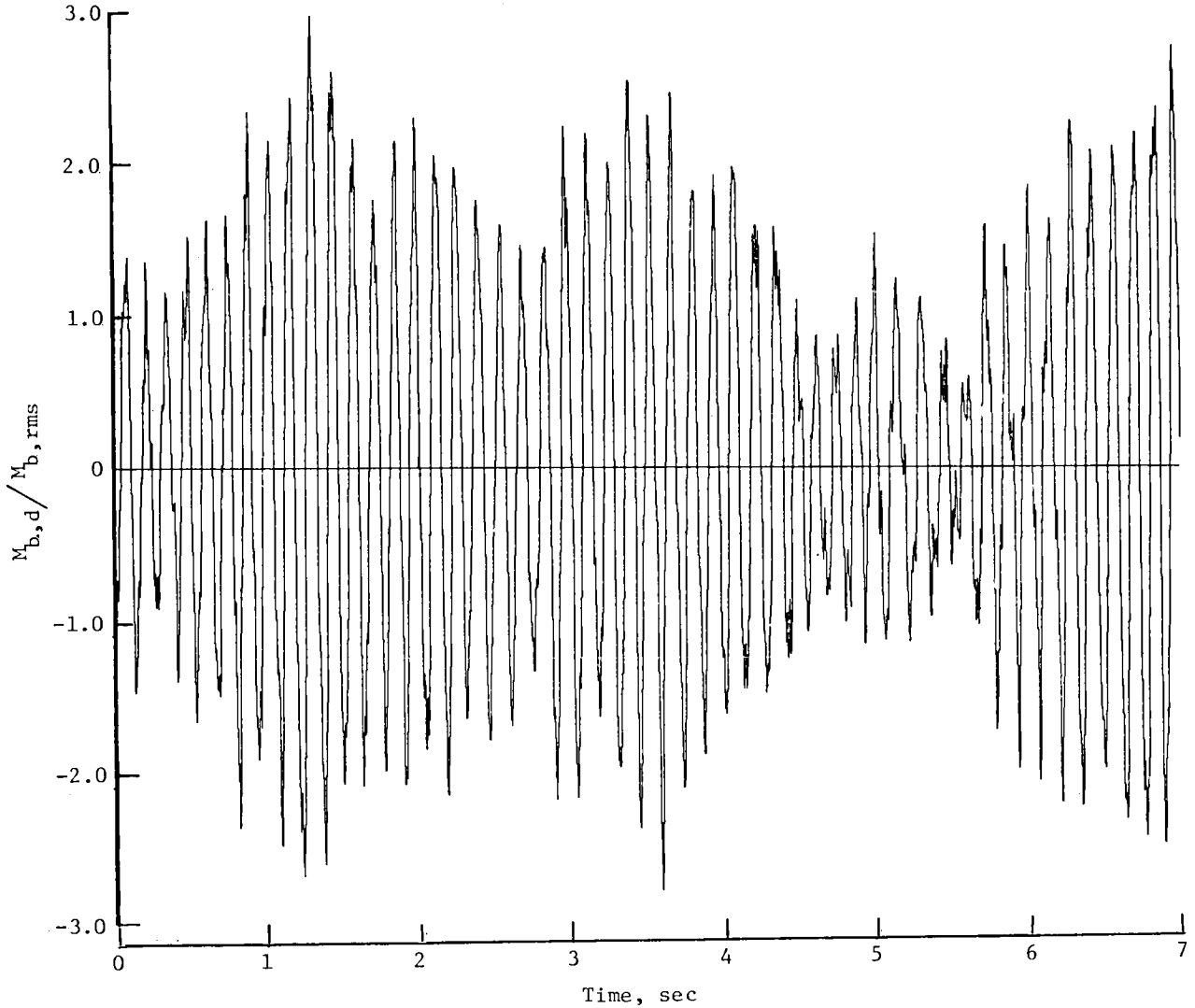

(b) $\alpha = 13^{\circ}$.

Figure 7.- Concluded.

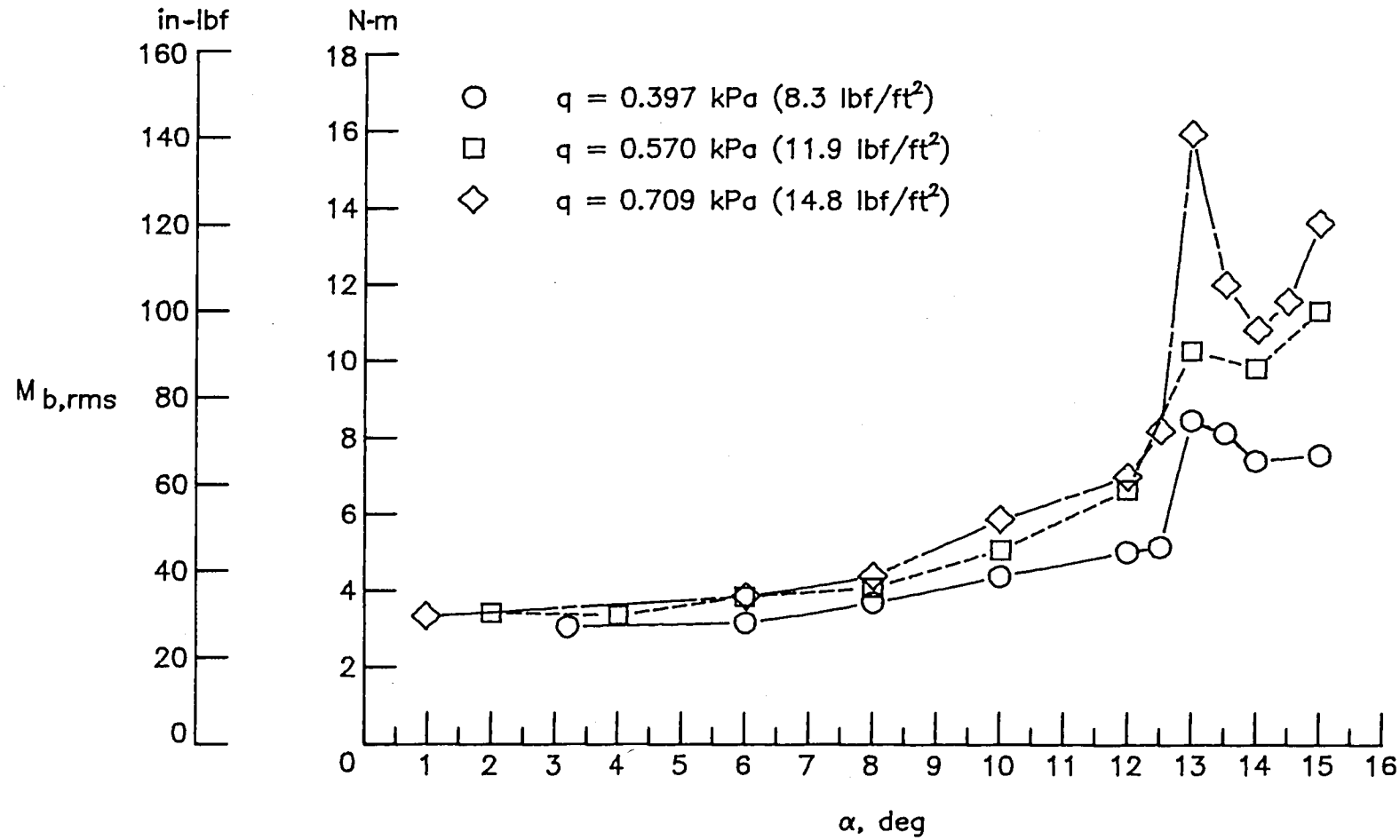

Figure 8.- Variation of broad-band rms bending moment with angle of attack.

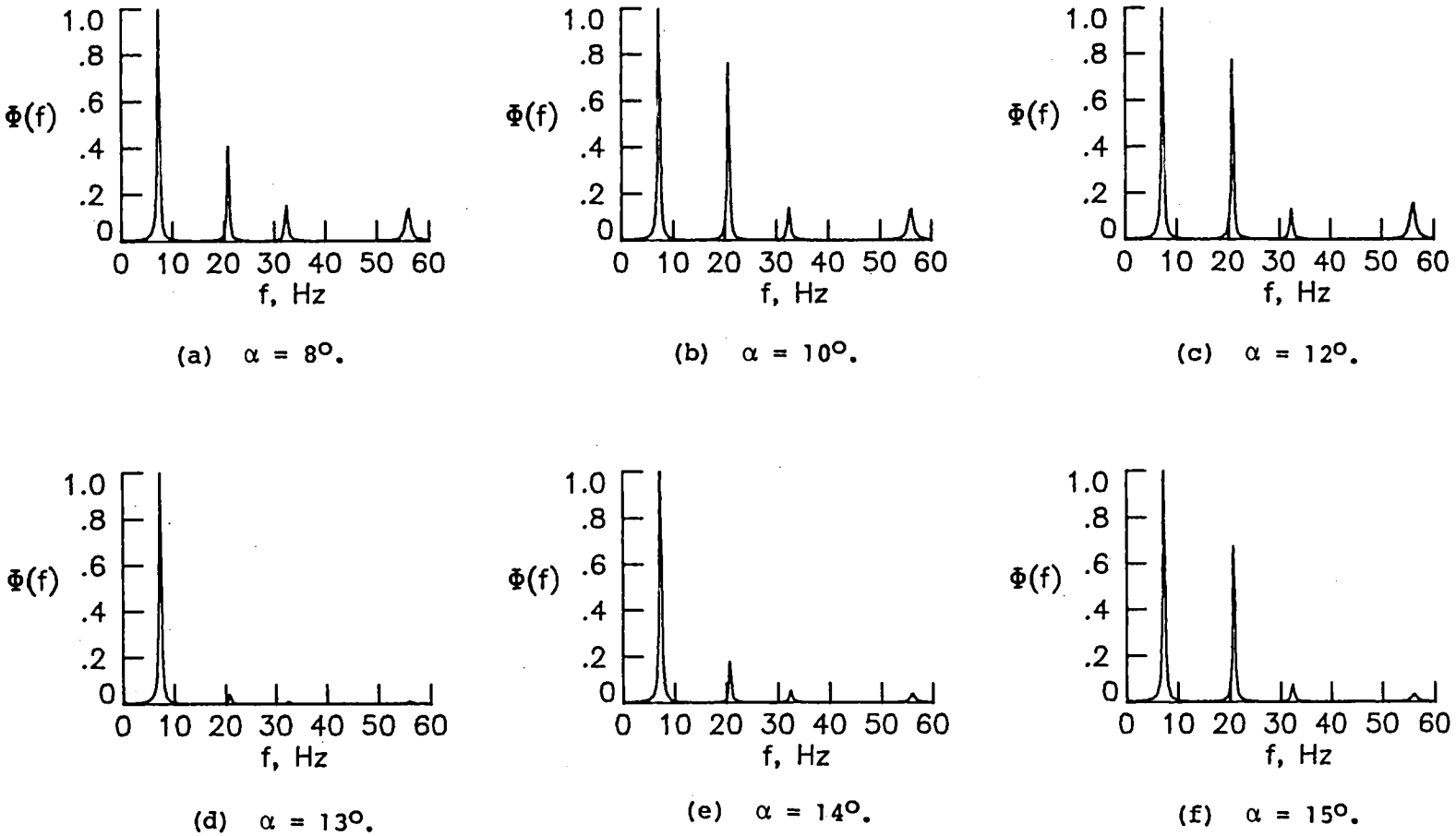

(a) $\alpha = 8^{\circ}$.

(b) $\alpha = 10^{\circ}$.

(c) $\alpha = 12^{\circ}$.

(d) $\alpha = 13^{\circ}$.

(e) $\alpha = 14^{\circ}$.

(f) $\alpha = 15^{\circ}$.

Figure 9.- Normalized autospectra. q = 0.709 kPa (14.8 lbf/ft^2).

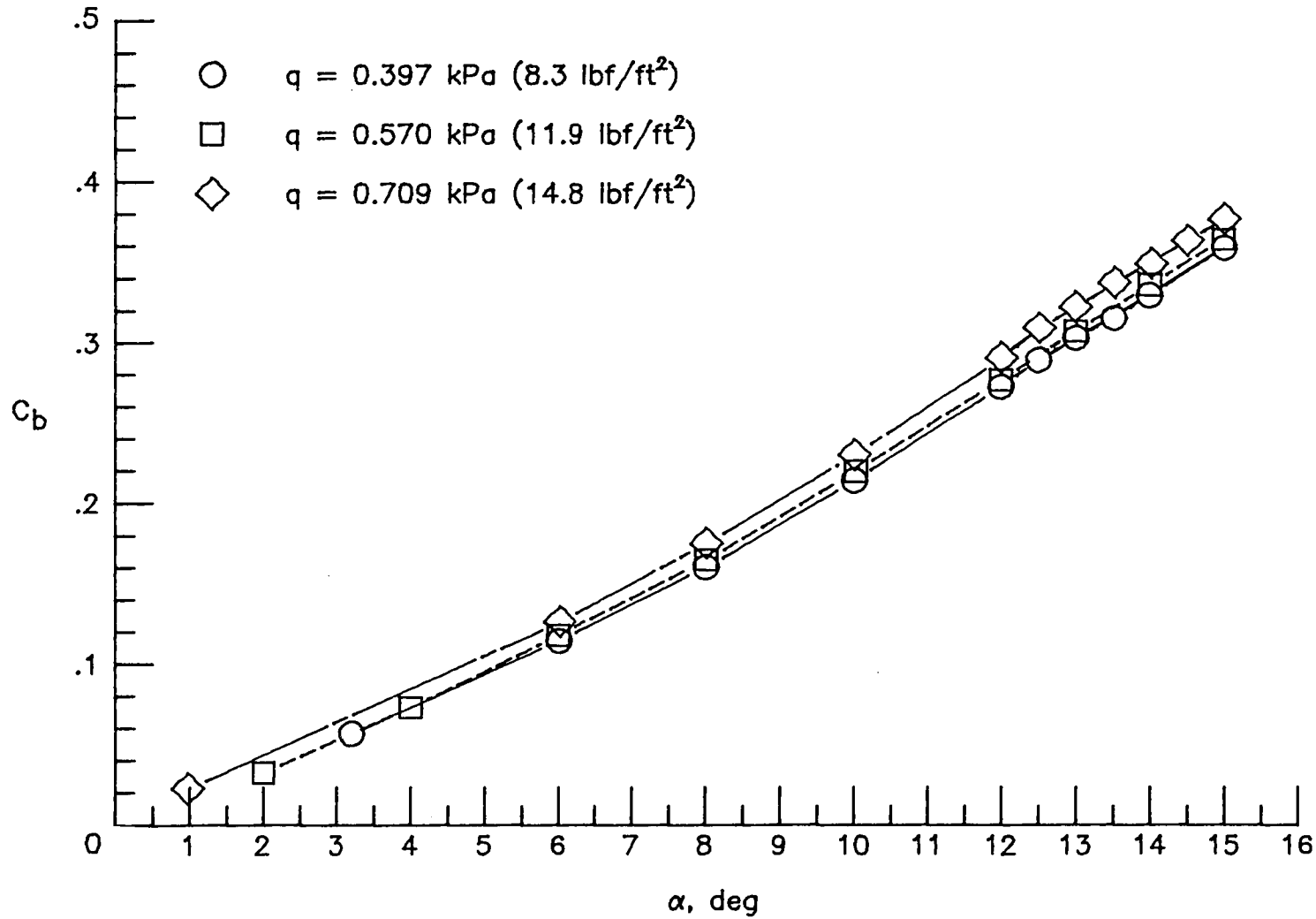

Figure 10.- Variation of static bending-moment coefficient with angle of attack.

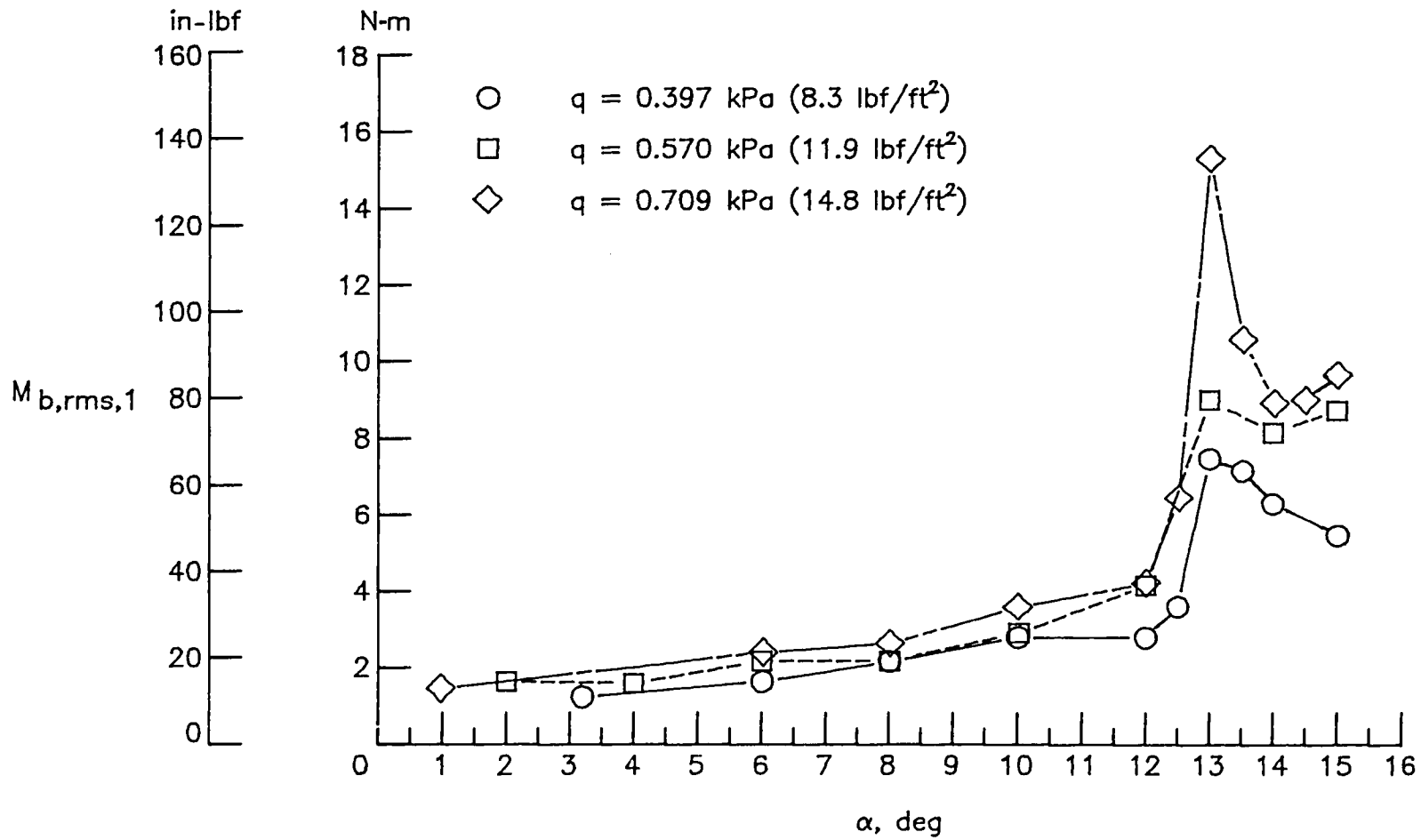

Figure 11.- Variation of rms bending moment for first mode with angle of attack.

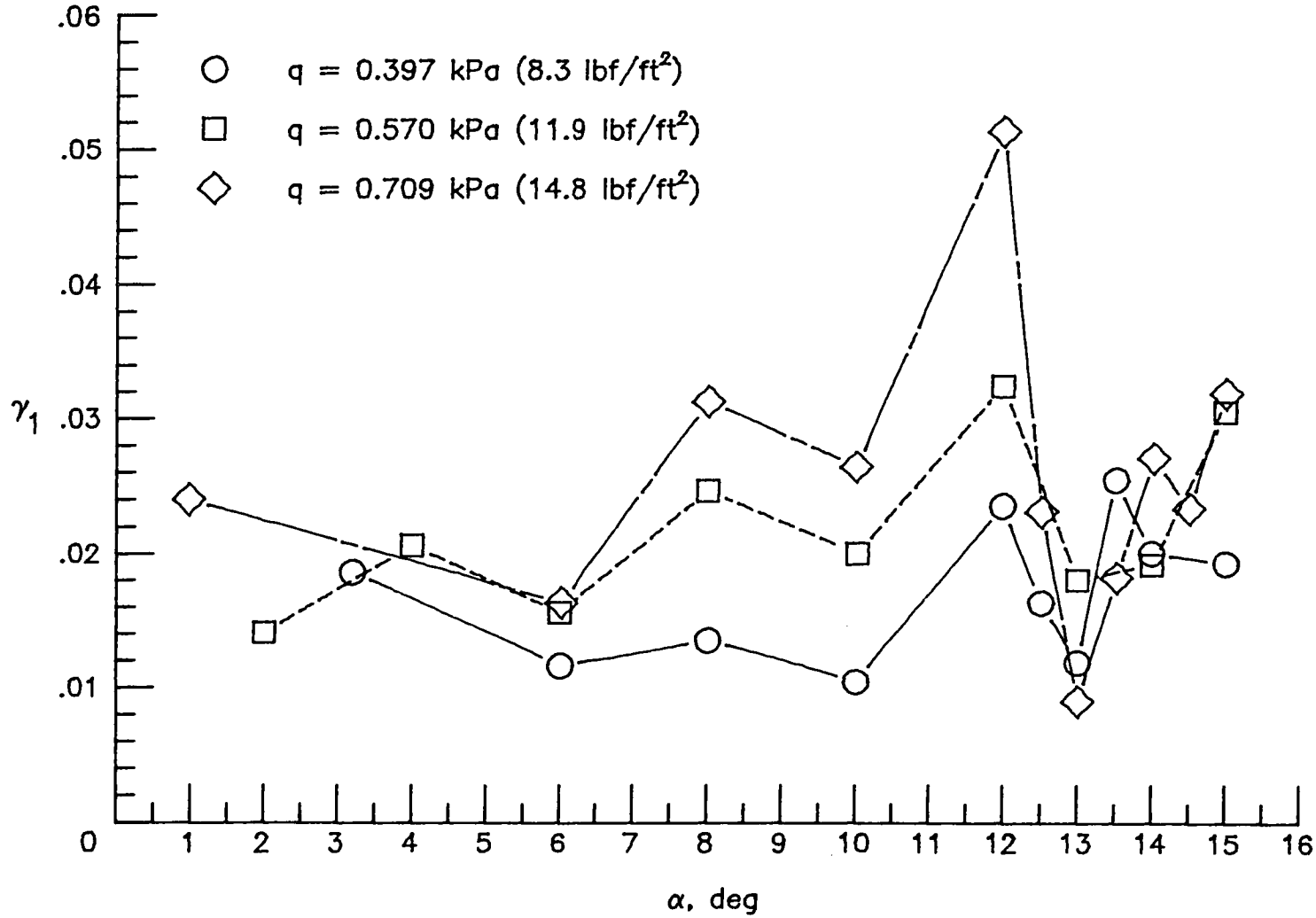

Figure 12.- Variation of total damping ratio for first mode with angle of attack.

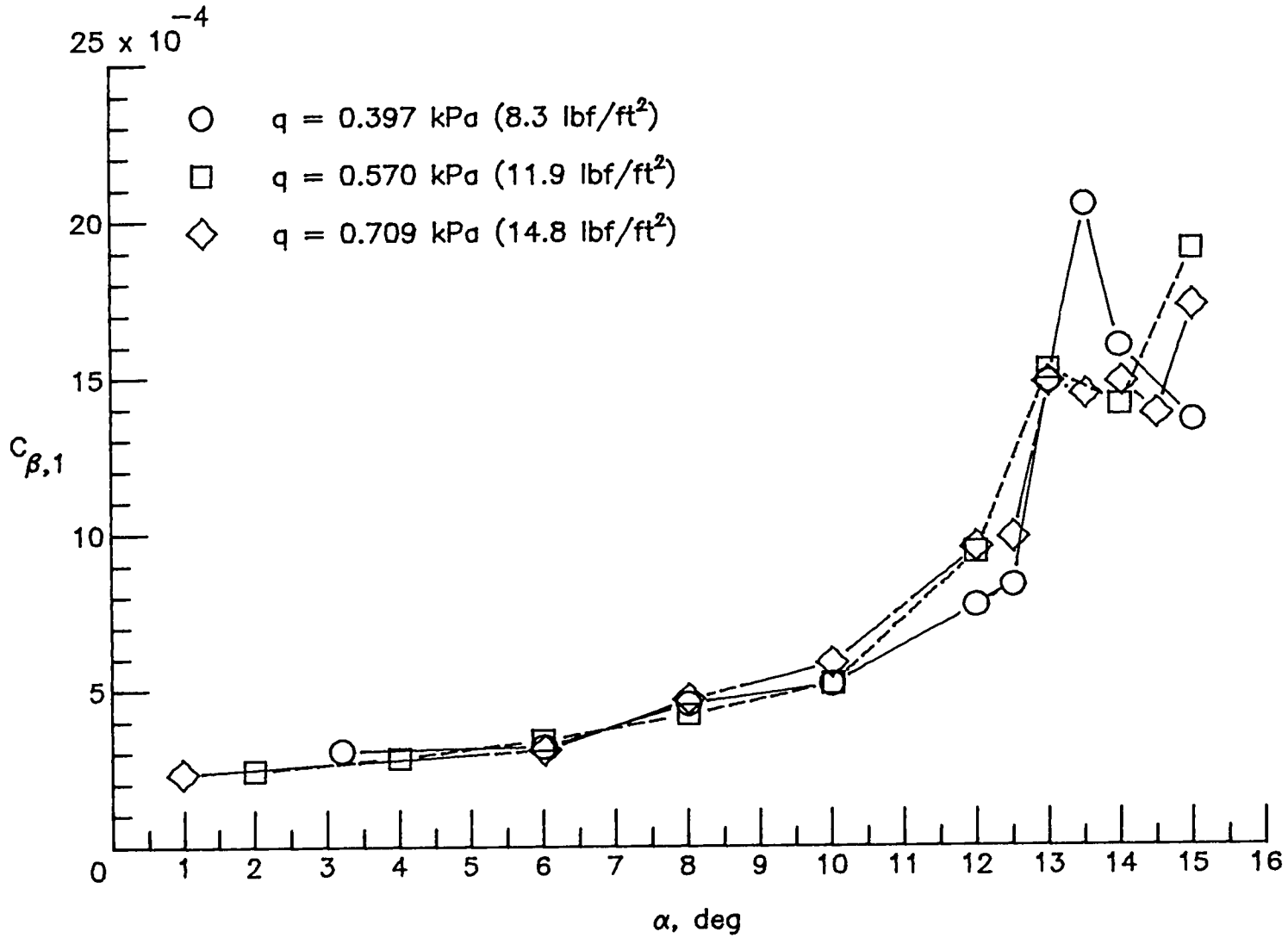

Figure 13.- Variation of buffet moment coefficient for first mode with angle of attack.

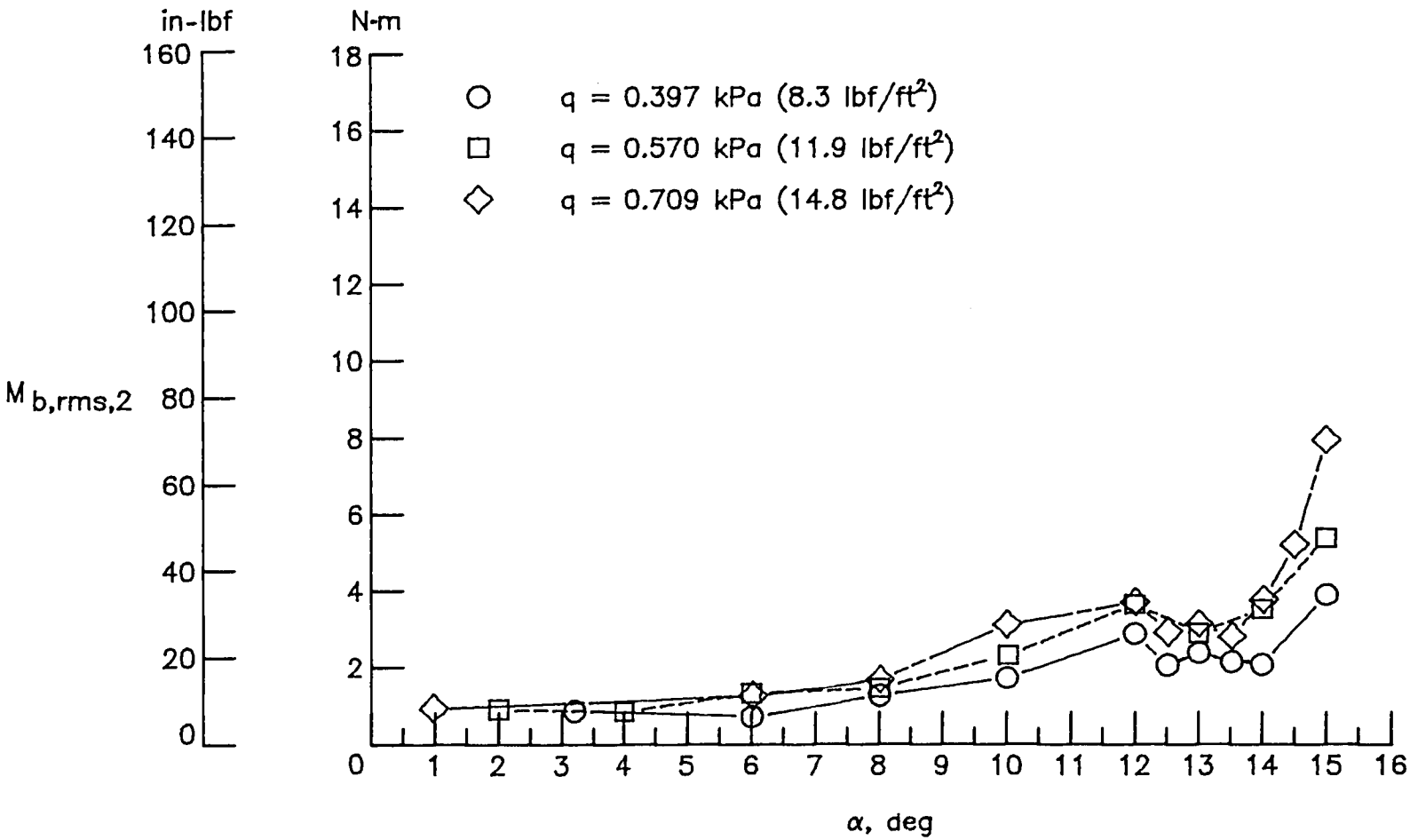

Figure 14.- Variation of rms bending moment for second mode with angle of attack.

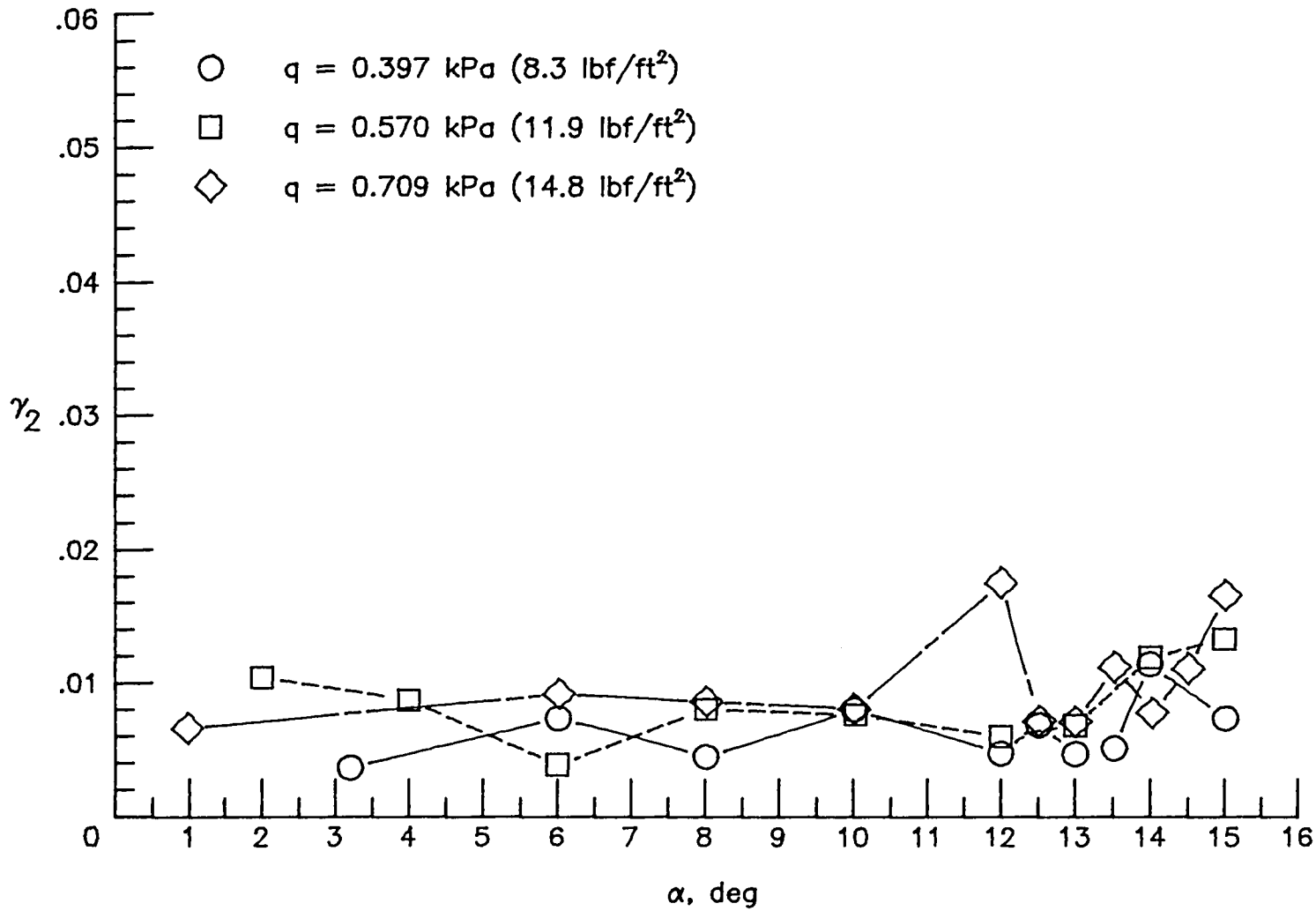

Figure 15.- Variation of total damping ratio for second mode with angle of attack.

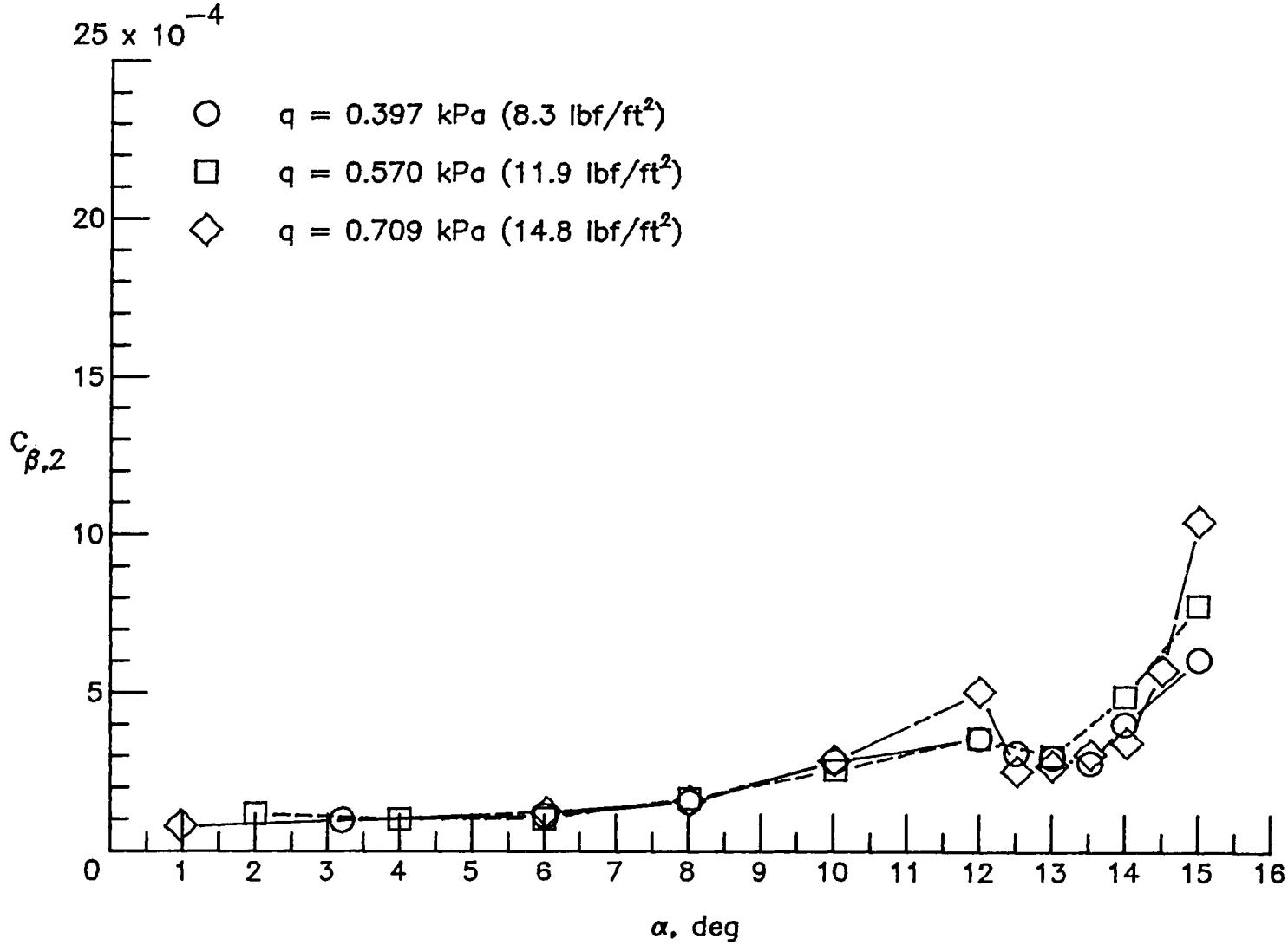

Figure 16.- Variation of buffet moment coefficient for second mode with angle of attack.

1. Report No.	2. Government Accession No.	3. Recipient's Catalog No.
NASA TM-81863		

4. Title and Subtitle	5. Report Date
DYNAMIC RESPONSE OF A FORWARD-SWEPT-WING MODEL AT ANGLES OF ATTACK UP TO 15° AT A MACH NUMBER OF 0.8	November 1980
	6. Performing Organization Code 505-43-33-01

7. Author(s)	8. Performing Organization Report No.
Robert V. Doggett, Jr., and Rodney H. Ricketts	L-13872
	10. Work Unit No.

9. Performing Organization Name and Address	11. Contract or Grant No.
NASA Langley Research Center Hampton, VA 23665	
	13. Type of Report and Period Covered

12. Sponsoring Agency Name and Address	13. Type of Report and Period Covered
National Aeronautics and Space Administration Washington, DC 20546	Technical Memorandum
	14. Sponsoring Agency Code

15. Supplementary Notes

16. Abstract

Root-mean-square (rms) bending moments for a dynamically scaled, aeroelastic wing of a proposed forward-swept-wing, flight-demonstrator airplane are presented for angles of attack up to 15° at a Mach number of 0.8. The 0.6-size semispan model had a leading-edge forward sweep of 44° and was constructed of composite material. In addition to broad-band responses, individual rms responses and total damping ratios are presented for the first two natural modes. The results show that the rms response increases with angle of attack and has a peak value at an angle of attack near 13°. In general, the response was characteristic of buffeting and similar to results often observed for aft-swept wings. At an angle of attack near 13°, however, the response had characteristics associated with approaching a dynamic instability, although no instability was observed over the range of parameters investigated.

17. Key Words (Suggested by Author(s))	18. Distribution Statement
Aeroelasticity Buffeting Dynamic response Forward-swept wings	Unclassified - Unlimited Subject Category 39

19. Security Classif. (of this report)	20. Security Classif. (of this page)	21. No. of Pages	22. Price
Unclassified	Unclassified	28	A03

N-305

For sale by the National Technical Information Service, Springfield, Virginia 22161

NASA-Langley, 1980

National Aeronautics and
Space Administration

Washington, D.C.
20546

Official Business
Penalty for Private Use, $300

THIRD-CLASS BULK RA[illegible]

[illegible]d
s and
n

U.S.MAIL

NASA

POSTMASTER: If Undeliverable (Section 158 Postal Manual) Do Not Return

LIBRARY MATERIAL SLIP
DO NOT REMOVE SLIP FROM MATERIAL
Delete your name from this slip when returning material to the library.

NAME	DATE	MS
~~FLORANCE, JAMES~~	~~2/14/2000~~	~~340~~

NASA Langley Form 474 (Rev. Oct. 1999)